Analytical Letters

ISSN: 0003-2719 (Print) 1532-236X (Online) Journal homepage: https://www.tandfonline.com/loi/lanl20

Determination of Nitrite Through *S*-Nitrosocaptopril Formation and Fluorescent Derivatization of Remaining Captopril Using *o*-Phthalaldehyde and Glycine

Youxin Li, Ying Zhang, Abd al-karim Ali & Neil D. Danielson

To cite this article: Youxin Li, Ying Zhang, Abd al-karim Ali & Neil D. Danielson (2019) Determination of Nitrite Through *S*-Nitrosocaptopril Formation and Fluorescent Derivatization of Remaining Captopril Using *o*-Phthalaldehyde and Glycine, Analytical Letters, 52:4, 649-670, DOI: 10.1080/00032719.2018.1484470

To link to this article: https://doi.org/10.1080/00032719.2018.1484470

Published online: 06 Aug 2018.

ANALYTICAL LETTERS
2019, VOL. 52, NO. 4, 649–670
https://doi.org/10.1080/00032719.2018.1484470

Taylor & Francis
Taylor & Francis Group

FLUORESCENCE

Determination of Nitrite Through *S*-Nitrosocaptopril Formation and Fluorescent Derivatization of Remaining Captopril Using *o*-Phthalaldehyde and Glycine

Youxin Li*, Ying Zhang, Abd al-karim Ali†, and Neil D. Danielson

Department of Chemistry and Biochemistry, Miami University, Oxford, OH, USA

ABSTRACT

We have developed an indirect fluorescence method for the determination of nitrite based on two reactions. The *S*-nitrosocaptopril produced by the first reaction between nitrite and excess captopril is not fluorescent. The fluorescent product produced by the residual captopril with glycine and *o*-phthalaldehyde is then measured and related to the nitrite concentration. We have optimized comprehensively the reaction condition parameters, including the thiol regent for the two reactions, reaction temperature and pH value for the first reaction, and the choice of amino acid, pH value, the ratio of reactants, buffer concentration, reaction temperature, and time for the second fluorescence reaction. Potential interferences by 8 cations and 10 anions on the fluorescence intensity were slight except for iodate and periodate which could likely be removed by addition of a reducing agent. For the analytical figures of merit, the limits of detection and quantitation of nitrite are 0.8 and 2.5 nM, respectively. The fluorescence intensity is found to linearly decrease with increasing nitrite from 0 to 140 nM. The method has shown to have good interday (<8%) and intraday precision (1–4%). The formation of nitrite from nitrate due to microbial degradation of spinach can be easily followed. Although the method requires a two-step reaction sequence that takes a significant analysis time, the safety and cost of the reagents (no carcinogenic amino naphthalene compounds) as well as excellent analytical figures of merit are significant advantages.

ARTICLE HISTORY
Received 16 August 2017
Accepted 31 May 2018

KEYWORDS
Captopril; fluorescence derivatizationglycine; glycine; nitrite; *o*-phthalaldehyde; spinach

Introduction

Nitrate is commonly used in fertilizers and as a food preservative, particularly in processed meat (Pandurangappa and Venkataramanappa 2011). If nitrite reacts with secondary amines, cancer suspect nitrosoamines can form. The "blue baby syndrome" and gastric cancer are the two main threats caused by excess nitrate and nitrite in drinking water (Bartsch, Hietanen, and Malaveille 1989). Both are the result from the reduced

CONTACT Neil D. Danielson danielnd@miamioh.edu Department of Chemistry and Biochemistry, Miami University, 651 E. High Street, Oxford, OH, 45056, USA
*Current address: Tianjin Key Laboratory for Modern Drug Delivery and High-Efficiency, Collaborative Innovation Center of Chemical Science and Engineering, School of Pharmaceutical Science and Technology, Tianjin University, Tianjin, China.
†Current address: Department of Chemistry, College of Education for Pure Science, Diyala University, Iraq.
Color versions of one or more of the figures in this article can be found online on at www.tandfonline.com/lanl.

oxygenation of the blood as irreversible conversion of hemoglobin to methemoglobin after the body converts nitrate to nitrite (Sobhanardakani et al. 2013). In order to minimize interferences in analytical methods, nitrite ion is usually allowed to undergo a nitrosation/diazotization reaction. The most common approach is the Griess assay, in which the nitrite is diazotized with sulfanilamide and then reacted with *N*-(1-naphthyl)ethylenediamine to form a colored product (Green et al. 1982).

A variety of chemical reactions have been evaluated for the fluorescent determination of nitrite (Wang et al. 2017). The reaction of 5-aminofluorescein with nitrite in acid to produce the highly fluorescent diazonium complex under basic conditions has been reported (Axelrod and Engel 1975). The detection limit of this method was about 50 pg/mL. A similar approach using 4-aminofluorescein reacted with nitrite to produce the highly fluorescent diazonium complex was been studied (Lapat, Szekelyhidi, and Hornyak 1997). However, few details are given and one possible limitation of this reaction might be the high reactant fluorescence background which could compromise detection of the fluorescent product. A fluorimetric procedure based on the cleavage reaction of nitrite with tryptophan was found to have a detection limit of 0.001 μg/mL (Jie, Yang, and Meng 1993). They also studied a new quenching method through the reaction of nitrite with the fluorescent indole to form a compound which has no fluorescence in acidic medium (Jie et al. 1999).

The non-fluorescent *N*-methyl-4-hydrazino-7-nitrobenzofurazan upon reaction with nitrite can be converted to the corresponding amino compound (Büldt and Karst 1999). A simple, sensitive and selective fluorimetric method is based on the reaction of acetaminophen with nitrite in an acidic medium to form a nitroso compound with a detection limit of 2.7 ng/mL (Helaleh and Korenaga 2000). Other fluorimetric methods based on the reaction of nitrite with rhodamine 110 to form a less fluorescent nitroso compound (Zhang et al. 2003) and with *o*-phenylenediamine (Guo et al. 2013) to form the fluorescent benzotriazole have also studied. Recently, using a synthesized rhodamine derivative, coupling of aniline and amide groups using nitrite to form the fluorescent benzotriazole rhodamine derivative has been characterized analytically (Cai et al. 2017).

The reaction of nitrite with 2,3-diaminonapthalene to form the more fluorescent naphthalene triazole derivative is well known (Wiersma 1970, Li, Meininger, and Wu 2000, Nussler et al. 2006). A variation based on the selective reaction of nitrite with 5,6-diamino-1,3-napthalene disulfonic acid in acidic medium to form a highly fluorescent compound 1-[H]-naphthotriazole-6,8-disulfonic acid has been reported to have a detection limit of 0.09 ng/mL (Wang et al. 2000). Recently, the reagent 4-amino-3-(1-methyl-1,2,3,4-tetrahydroquinolin-7-yl)benzonitrile has been synthesized and upon reaction with nitrite under acidic conditions cyclizes through the primary amine group to complete a fused ring structure which has both a significant bathochromic shift and is highly fluorescent (Shen et al. 2015). A limit of detection of 2.6 nM with linearity to 100 nm was reported. Most of these fluorescent methods involve the use of cancer suspect compounds such as aminonaphthalene derivatives (Radomski et al. 1971, Sugimura 2000, Material Safety Data Sheet, 2017). Some of the previously cited derivatizing agents, particularly the diaminonaphthalene reagents, are expensive, on the order of several hundreds of dollars per g.

The reaction of *o*-phthalaldehyde, a thiol compound, and a primary amine at alkaline pH to form the fluorescent isoindole derivative is one of the most important analytical approaches for the determination of amino acids and selected pharmaceuticals. Interestingly, indoles such as the isoindole indole-3-carbinol have been found to possess anti-tumor activity, particularly if prolonged ingestion is not required (Dashwood 1998, Higdon et al. 2007). Captopril, (2*S*)-1-1[(2*S*)-3-mercapto-2-methylpropanoyl] pyrolidine-2 carboxylic acid, is an inhibitor of angiotensin and could be used as the thiol compound in the *o*-phthalaldehyde reaction (Kok et al. 1997). The excitation and emission wavelengths were set at 345 and 455 nm. The best solution condition for this reaction was with 0.1 M borate buffer (pH 7.5). The limit of detection for captopril was 50 pg/mL in human plasma and 250 ng/mL in urine. Linear calibration curves could be obtained at the low nanogram range. We have shown that captopril can react with nitrite at acidic pH to generate nitrosocaptopril and be detected by absorbance at 333 nm (Scaffidi et al. 2015). The reaction is fast, suitable for flow injection analysis, but the sensitivity is quite low.

To the best of our knowledge, a new approach has been developed in this study using captopril with fluorescence detection to determine the nitrite concentration indirectly. The first reaction occurs between nitrite and captopril at acidic pH to generate *S*-nitrosocaptopril. A small volume of this solution is added to the borate buffered OPA and glycine solution, and the resulting mixture will produce a fluorescent signal if captopril remains from the first reaction. The two reaction scheme is shown in Figure 1. Aqueous solutions of nitrite can produce two nitrosating agents: NO^+ and N_2O_3. The pseudo first-order rate constant for *S*-nitrosocaptopril formation under strong acid conditions depends first order on $[NO^+]$ plus second order on $[N_2O_3]$. At low nitrite concentrations (<15 mM), nitrosation of captopril is dominated by NO^+ (Sexto and Iglesias 2011). The second reaction of OPA and a primary amine at alkaline pH with the remaining captopril produces a fluorescent isoindole derivative and the sensitivity to detect nitrite is expected to be markedly improved. The fluorescent signal is proportional to the remaining concentration of captopril after the first reaction and sub-nM levels of nitrite can be detected if the analysis time is long. The presence of nitrite in environmental water samples as well as the formation of nitrite from nitrate due to microbial degradation of spinach could be easily measured.

Experimental

All fluorescence measurements were performed on a Perkin-Elmer model LS 55 fluorescence spectrometer (Waltham, MA). The excitation wavelength and slit were set to 345 and 10 nm, respectively. The emission wavelength was scanned from 350 to 600 nm and the slit was set to 10 nm. The scan speed was 500 nm per min. When *N*-acetyl-L-cysteine, captopril, or 3-mercaptopropionic acid was used as the thiol regent, the maximum emission wavelength for the fluorescent reaction product was selected at 447, 450, and 454 nm, respectively. A 4 mL quartz cuvette of 1 cm light-path was used for the emission measurements. The cell temperature could be adjusted from 4 to 60 °C, which was controlled by circulating water from a Fisher model 730 Isotemp Immersion Circulator.

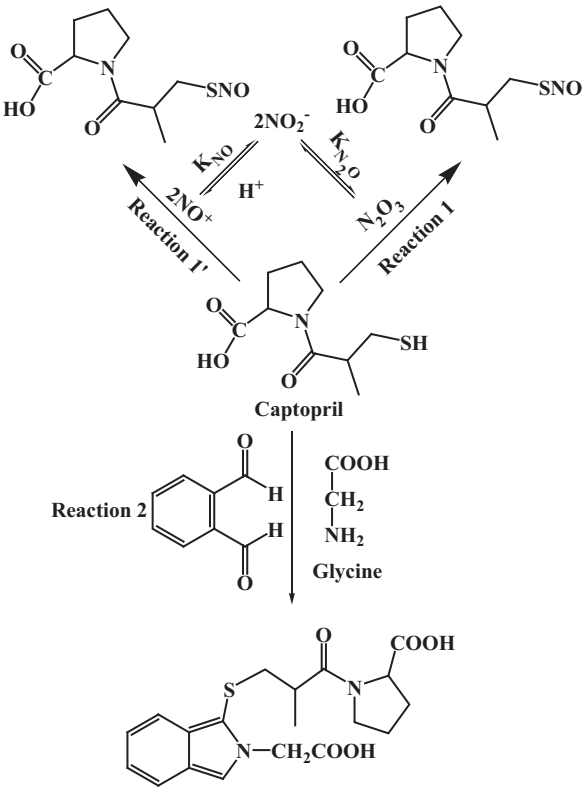

Figure 1. Two reaction pathways (1 and 1′) for captopril and nitrite. Reaction 2 involved captopril, *o*-phthalaldehyde and glycine.

The temperature of the sample solution was held at 0 °C in an ice bath. Data were recorded and analyzed using the FL WinLab software V 4.00.03. Standard ultraviolet-visible absorbance measurements were carried on a Hewlett Packard 8453 ultraviolet-visible spectrophotometer (Santa Clara, CA) and all samples were scanned from 200 to 600 nm. When 3-mercaptopropionic acid, captopril, or *N*-acetyl-L-cysteine was used as the thiol regent, the maximum absorbance wavelengths for the reaction product were selected to be 329, 332, and 334 nm, respectively. All pH measurements were monitored by a Thermo Scientific Orion 2 Star pH meter with an automatic temperature compensation epoxy probe from Fisher Scientific (Pittsburgh, PA). A Branson 2510 ultrasonic cleaner (Danbury, CT) was used to assist the dissolution of sodium tetraborate decahydrate.

Chemicals

Unless otherwise noted, all chemicals were of analytical grade or better. Captopril, *N*-acetyl-L-cysteine, 3-mercaptopropionic acid, alanine, arginine, asparagine, aspartic acid, cystine, glutamic acid, glycine, isoleucine, leucine, lysine, methionine, phenylalanine, serine, threonine and valine of HPLC grade (99% or higher) were obtained from Sigma-Aldrich (St. Louis, MO). *o*-Phthalicdicarboxaldehyde, more commonly known as *o*-phthalaldehyde, as HPLC grade (99% or higher), sodium tetraborate decahydrate, and

sodium bromide were from Aldrich (Milwaukee, WI). Methanol (HPLC grade), sulfuric acid, sodium hydroxide, sodium nitrate, potassium nitrate, lead nitrate, magnesium nitrate hexahydrate, calcium nitrate tetrahydrate, zinc nitrate hexahydrate, ferric nitrate nonahydrate, sodium iodide, sodium iodate, sodium perchlorate, sodium sulfite, sodium sulfate, sodium thiosulfate and sodium phosphate were from Fisher Scientific.

The sodium chloride was from VWR (Batavia, IL). Sodium nitrite was from Tedia (Fairfield, OH). Strontium nitrate was from J. T. Baker Chemical Co. (Phillipsburg, NJ). Sodium periodate was from Spectrum Chemical (Gardena, CA). Distilled deionized water was supplied using a Millipore MilliQ filtration system (Dubuque, IA) to a purity of 18.2 MΩ resistivity. The stock solution was prepared by adding a certain amount of methanol to assist dissolution of the *o*-phthalaldehyde in distilled deionized water before dilution of the stock solution with water to make the standard assay solution. Cystine required dissolution in dilute sodium hydroxide solution before dilution with distilled deionized water. Sodium hydroxide (NaOH) solution (10.42 M), which was used to adjust the pH value, was prepared by dissolving 25 g sodium hydroxide solid in 60 mL water. All of the other solutions, such as captopril, sodium nitrite and glycine, were prepared with distilled deionized water.

Methods

The monitored fluorescence was from the product of the second reaction involving the remaining captopril, *o*-phthalaldehyde, and glycine at basic pH conditions. The detailed experimental steps follow.

Procedure 1

The pH value of the sample solution containing nitrite was adjusted to 1.00 by addition of sulfuric acid. A 9.44 mL volume of the solution was put into a glass tube, capped and preheated to 40 °C in water bath. A 100 μL volume of 15 μM captopril was added to the above solution and the reaction was maintained for 40 min at 40 °C. Second, a 260 μL volume of 10.42 M NaOH stock solution and a 0.3814 g mass of $Na_2B_4O_7{\cdot}10H_2O$ solid were added to the solution to reach the final pH 9.50. Third, a 100 μL volume of 15 μM *o*-phthalaldehyde and a 100 μL volume of 15 μM glycine were added to the above solution and mixed to start the second reaction for 24 h (or at least overnight) at 10 °C. Last, the fluorescence signal of the product was scanned and recorded.

Procedure 2

The conversion of nitrate to nitrite in spinach was performed using this procedure. Because the necessity of a low detection limit is not of concern for this sample, this procedure is more facile than procedure one. A 400 gram amount of fresh clean non-organic spinach from a local supermarket was placed in a blender, followed by the addition of 400 mL of distilled deionized water, and then homogenized for 3 min until it was converted into juice. The spinach juice was transferred to 1 L volumetric flask and diluted to the mark. A 10 mL portion, taken from spinach juice after standing at ambient temperature for 0, 3, 6, 12, 18, 24, 30, 36, 42, 48, 54, and 60 h, was after blending,

mixed with 1 mL of 0.01 M NaOH to stop the microorganisms from producing more nitrite, and kept in the refrigerator for storage before analysis.

The reaction between nitrite and captopril was carried under acidic conditions at pH 1 using sulfuric acid. A 1 mL volume of each nitrite standard or sample was placed into a 50 mL volumetric flask and then mixed with 2 mL of 8 ppm captopril (3.69×10^{-5}M), followed by 3 mL of 0.1 M H_2SO_4. The mixture was left for 15 min to ensure the completion at room temperature. For the fluorescent reaction between the remaining captopril, *o*-phthalaldehyde, and glycine, a 25 mL volume of 0.09 M pH 9.00 borate buffer was added to the previous mixture. Then 2 mL of 10 ppm *o*-phthalaldehyde was added followed by another 2 mL of 10 ppm of glycine; the final volume was brought up to 50 mL. This mixture was left for 2 h at room temperature before measurement of the fluorescence signal. The total analysis time using this procedure was 2 hr and 15 min.

Results and discussion

Selection of the thiol and amine reagents

The thiol compound chosen for this study is important because it has a dual role: reaction first with nitrite and then with the fluorescent reagent. Thus, a fluorescent reagent which can react with a thiol group must be selected. There are many commonly used reagents, like 7-fluoro-2,1,3-benzoxadiazole-4-sulfonamide (Ogasawara et al. 2007), 7-fluorobenzo-2-oxa-1,3-diazoloe-4-sulfonamide (Nolin, McMenamin, and Himmelfarb 2007), *o*-phthaldialdehyde (Mukai et al. 2002), and 5-methyl-(2-(m-iodoacetylaminophenyl)benzoxazole (Liang et al. 2005). Most of these reagents have a high sensitivity. However, some reagents are not totally satisfactory. For 7-fluoro-2,1,3-benzoxadiazole-4-sulfonamide and 7-fluorobenzo-2-oxa-1,3-diazoloe-4-sulfonamide, it is necessary to run the reaction at a high derivatization temperature. For 5-methyl-(2-(m-iodoacetylaminophenyl)benzoxazole, the product has to be determined at a short wavelength of difference $\lambda_{ex}/\lambda_{em}$, which is not compatible with our instrument. The detection limit of coenzyme A containing a thiol group when reacted with a new derivatizing reagent, 1,3,5,7-tetramethyl-8-phenyl-(4-iodoacetamido) difluoroboradiaza-s-indacene was found to be 1.8 fmol (Guo et al. 2009). However, this reagent was designed and synthesized in their lab and is not commercially available. Thus, commercially available *o*-phthalaldehyde was chosen as the derivatizing reagent to be reacted with the excess remaining thiol compound.

D- and L-alpha-amino acids in foods and beverages by precolumn derivatization with *o*-phthalaldehyde combined with the chiral thiol *N*-isobutyryl-L-cysteine or its enantiomer *N*-isobutyryl-D-cysteine have been determined (Brückner et al. 1995). Being chiral, these cysteine reagents are very expensive and a more common compound must be considered as the thiol agent for the reaction with *o*-phthalaldehyde and nitrite. Three kinds of thiol reagents, including *N*-acetyl-L-cysteine, 3-mercaptopropionic acid, and captopril were selected as thiol regents. All have previously been used for OPA fluorescence detection for amino acids. The ultraviolet absorbance spectra for these three S-nitrosylation products are shown in Figure 2.

Captopril, *N*-acetyl-L-cysteine, and 3-mercaptopropionic acid were able to react with nitrite and the reaction could be completed in 8, 10, and 12 min (Figure 3), respectively.

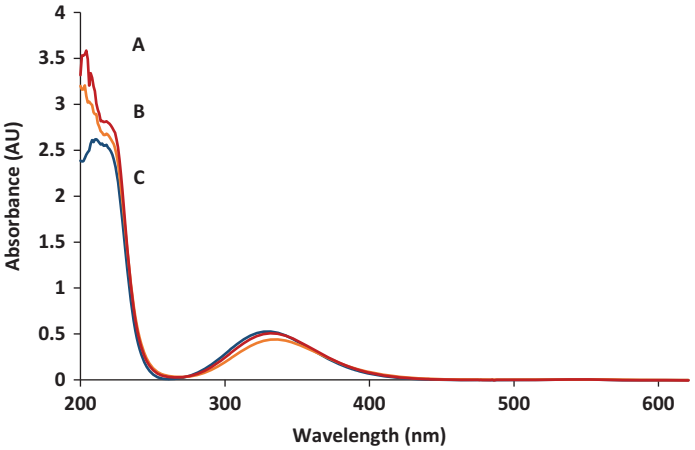

Figure 2. Ultraviolet spectra of three products produced by reacting (A) 500 μM nitrite and 500 μM captopril (red, at 220 nm), (B) 500 μM nitrite and 500 μM N-acetyl-L-cysteine (orange, at 220 nm), and (C) 500 μM nitrite and 500 μM 3-mercaptopropionic acid (blue, at 220 nm). Spectra from top to bottom at 330 nm are nitrite-3-mercaptopropionic acid, nitrite-captopril, and nitrite-*N*-acetyl-L-cysteine.

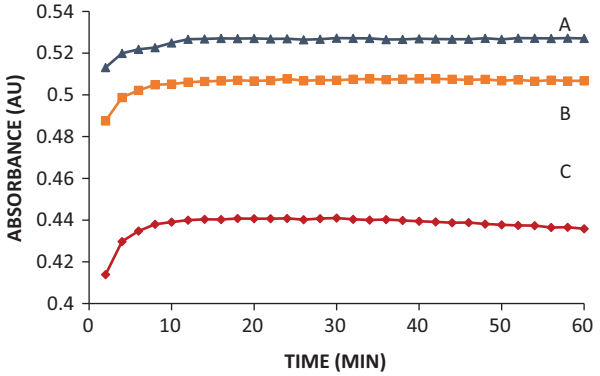

Figure 3. Ultraviolet absorbance signals of three products produced by reacting (A) 500 μM nitrite and 500 μM 3-mercaptopropionic acid (blue triangles) at 329 nm, (B) 500 μM nitrite and 500 μM captopril (orange squares) at 332 nm, and (C) 500 μM nitrite and 500 μM *N*-acetyl-L-cysteine (red diamonds) at 343 nm all at pH 1 as a function of time.

All three thiol regents undergo ultraviolet absorbance in the 330 nm range after reaction with nitrite. 3-Mercaptopropionic acid produced the highest absorbance signal compared to *N*-acetyl-L-cysteine and captopril under the same conditions. Slightly different absorptivities and maximum absorption peak wavelengths are observed. The molar absorptivities of the S-nitroso products of *N*-acetyl-L-cysteine, 3-mercaptopropionic acid, and captopril are 882, 1054, and 1,015 $M^{-1} \cdot cm^{-1}$, respectively. The result for *S*-nitroso captopril is basically the same as the literature value (Sexto and Iglesias 2011). The molar absorptivity is related to the carboxyl group and the acylamino group and its relative position, which also affect their maximum wavelengths attributed to the allowed

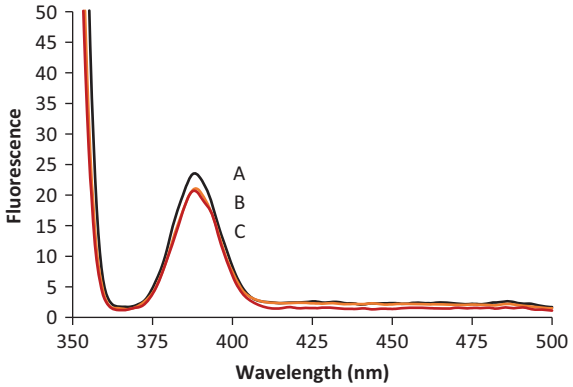

Figure 4. Fluorescence spectra of three products produced by reacting (A) 500 μM nitrite-500 μM *N*-acetyl-L-cysteine (black), (B) 500 μM nitrite – 500 μM captopril (orange), and (C) 500 μM nitrite – 500 μM 3-mercaptopropionic acid (red).

$n_o \rightarrow \pi^*$ transition at 334, 329 and 332 nm for each of S-nitroso products of *N*-acetyl-L-cysteine, 3-mercaptopropionic acid, and captopril, respectively.

The fluorescent spectra of three products produced by reacting nitrite and each of the three thiol reactants are shown in Figure 4. As expected, the response is weak and there is no signal for three S-nitrosylation products over a wavelength range of 425–600 nm. This is important since the *o*-phthalaldehyde-thiol-primary amine isoindole product is expected to fluoresce in this range.

Previously, isoleucine has been used for the *o*-phthalaldehyde – thiol derivatization reaction (Concha-Herrera, Torres-Lapasio, and Garcia-Alvarez-Coque 2004) but no comprehensive comparison to other amino acids was done. In the presence of captopril, the fluorescence of the l-alkylthio-2-alkylisoindole generated by the reaction of *o*-phthalaldehyde with the primary amine group derived from 15 amino acids, including cystine, aspartic acid, isoleucine, valine, glutamic acid, phenylalanine, methionine, alanine, leucine, threonine, arginine, asparagine, lysine, serine and glycine were studied. Comparison of the fluorescence signals are shown in Figure 5. The results indicated that the fluorescence reaction is faster and more sensitive when the α-carbon of the amino acid has none or a small group substitute, or small group substituent, like glycine and serine. For some reason, alanine does not follow this trend. Although there could be formation of two different l-alkylthio-2-alkylisoindole with an amino acid containing two NH_2 groups, *o*-phthalaldehyde is sensitive to those bifunctional amino acids, like arginine, lysine, and asparagine except cystine, which delivered the lowest fluorescence signal. That may be due to a competitive reaction because of the SH group generated by the hydrolysis of cystine in a basic solution. There was no significant difference when *o*-phthalaldehyde and captopril were reacted with the other amino acids. Taking the fluorescence intensity into account, glycine was chosen as the primary amine reactant for the following optimization experiments.

To finalize the reagents for the indirect method for nitrite determination, the reaction of each thiol with *o*-phthalaldehyde and glycine was compared as a function of time as shown in Figure 6(A). Captopril was chosen as the thiol reactant because it had the

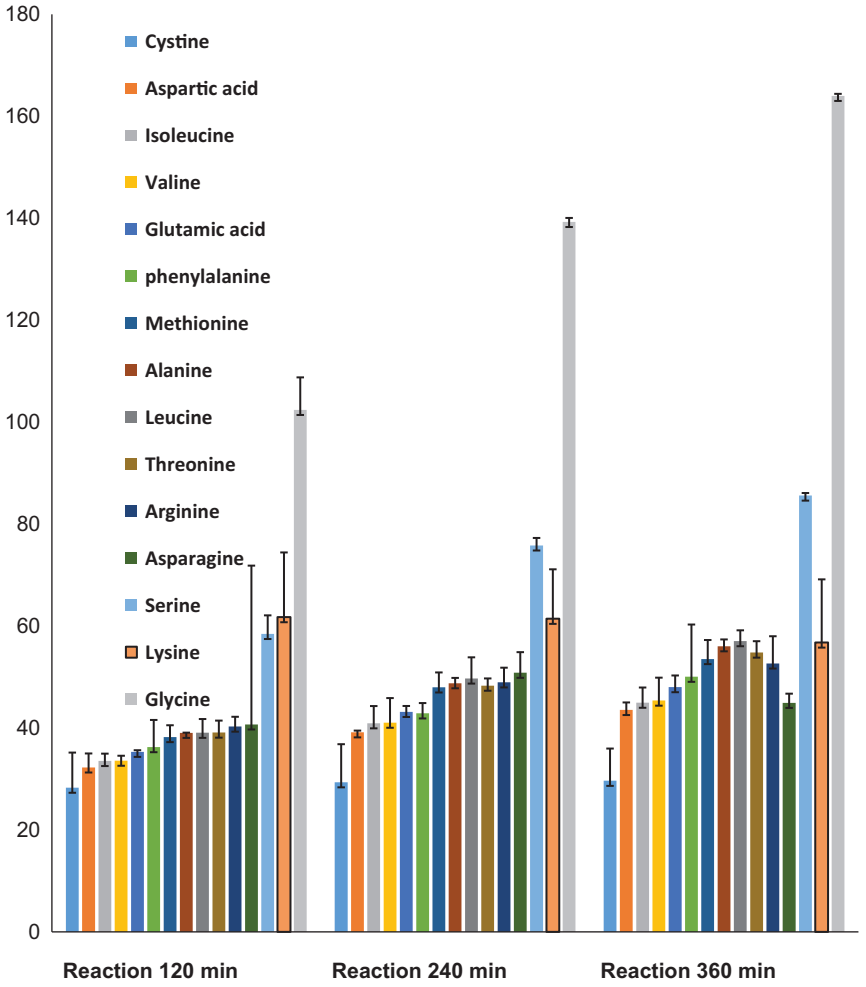

Figure 5. Fluorescence response comparison of amino acids with *o*-phthalaldehyde and captopril as a function of time. Left to right: cysteine, aspartic acid, isoleucine, valine, glutamic acid, phenylalanine, methionine, alanine, leucine, threonine, arginine, asparagine, lysine, serine, and glycine.

highest fluorescence signal (Figure 6(B)). However, the optimum reaction time is quite long, on the order of hours for the maximum fluorescence signal.

Optimization of pH and temperature for reaction 1

For the formation of nitrosocaptopril, the influence of $[H^+]$ is very important because the nitrite ion is not a nitrosating agent in basic medium (Sexto and Iglesias 2011). Meanwhile, in strong acid medium, nitrite is in the form of HNO_2, which is easy to form NO^+, because the pK_a of this weak acid is 3.14 at 25 °C. It means that the overall nitrite concentration is the sum of nitrite ion and nitrous acid when the pH value is more than 2.5 and the reaction rate will dramatically reduce as the pH increases above 3.2. Thus, the intensity of $[H^+]$ directly affects the formation rate of NO^+ and the reaction rate of the nitrosation of captopril. In addition, the pH also affects the extent of

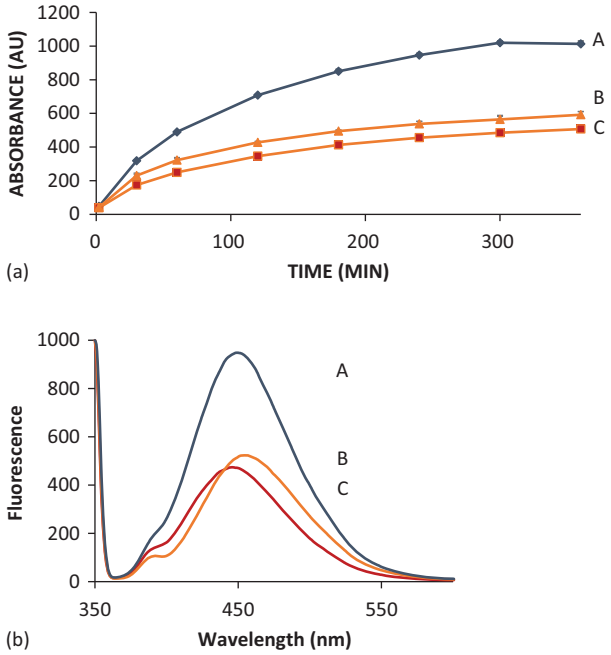

Figure 6. (A) Fluorescence of three products produced from 1 μM *o*-phthalaldehyde – 1 μM glycine – 1 μM captopril at 450 nm (A, blue diamonds); 1 μM *o*-phthalaldehyde – 1 μM glycine – 1 μM 3-mercaptopropionic acid at 454 nm (B, orange triangles); and 1 μM *o*-phthalaldehyde – 1 μM glycine – 1 μM N-acetyl-L-cysteine at 447 nm (C, red squares) as a function of time. (B) Corresponding fluorescence emission spectra of products A, B, and C from Figure 6(A).

the ionic or neutral form of captopril, because the pKa of the carboxylic group is 3.52. Therefore, the effect of pH over a range from 1 to 4 on the reaction rate between captopril and nitrite was investigated. The data were recorded at each 2 min interval and the signal-time profiles are shown in Figure 7(A).

The fastest reaction was completed in 6–8 min at pH 1, but the time was more than 25 min at pH 2. Especially, at pH 3, the reaction did not quite go to completion during the monitored 60 min. At pH 4, the ultraviolet absorbance has little increase beyond 30 min. This could be easily interpreted according to the reaction and decomposition rate of the *S*-nitrosocaptopril because it is not stable in a basic medium. In strong acid situation, like pH 1, the reaction rate is so fast that the decomposition could be negligible. However, at pH 4, the reaction rate is fast in the beginning step and then formation-decomposition gradually achieve on equilibrium. The data indicated that the fastest reaction rate and the least decomposition could be obtained at pH 1.

To our best knowledge, there are few studies of the temperature effect on the S-nitroso reaction involving nitrite and a thiol regent, especial the reaction between nitrite and captopril. In this study, the ultraviolet absorbance of the reaction was studied at 20, 30, 40 and 50 °C. The chronological measurements were recorded at each minute interval as shown in Figure 7(B). The reaction time was shortened from 20 to 6 min with the increase of the temperature from 20 °C to 50 °C. The reaction was consistent at 40 and 50 °C. The slight decrease of the absorbance value at 20 °C suggests there was

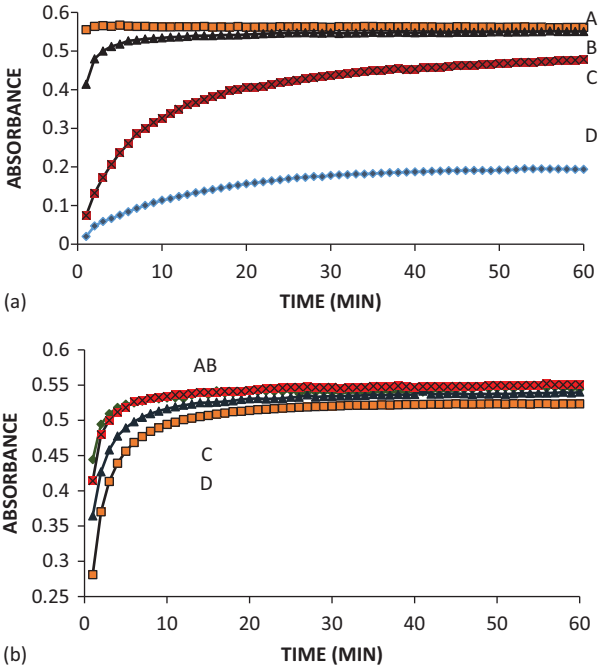

Figure 7. Nitrite and captopril reaction as a function of time: (A) pH optimization at 40 °C: A orange pH 1; B black pH 2; C red pH 3; and D blue pH 4. (B) Temperature optimization: A green 50 °C, B red 40 °C, C blue 30 °C, and D orange 20 °C.

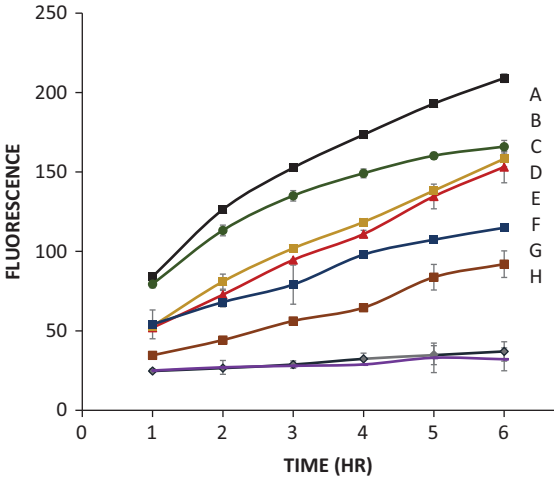

Figure 8. pH optimization for the *o*-phthalaldehyde, captopril, glycine fluorescence reaction. pH values: (A) black squares 9.50, (B) green circles 10.01, (C) yellow squares 9.01, (D) red triangles 8.51, (E) blue squares 11.01, (F) brown squares 8.01, (G) gray diamonds 7.01, and (H) purple points 12.02.

a tiny increase in decomposition of *S*-nitrosocaptopril. Hence, 40 °C is to be considered as the optimum reaction temperature.

Optimization of fluorescence reaction 2 conditions

There are two reports focused on the determination of captopril in biological media by HPLC separation with fluorescence detection after pre-column derivatization with glycine and *o*-phthalaldehyde (Kok et al. 1997, Hadjmohammadi, Kamel, and Nezhad 2008]. In this study, to further optimize the OPA derivatization procedure for captopril, the ratio of reactants, buffer concentration, as well as pH, temperature, and reaction time were investigated.

A very important parameter for the derivatization reaction and stability of the adduct is the pH. The effect of pH on the time course of the *o*-phthalaldehyde induced fluorescence reaction was investigated with other conditions fixed constant. As shown in Figure 8, the pH was adjusted from 7.01 to 12.02 using 0.06 M borate buffer. As expected, the results indicated that the derivatization reaction is pH-dependent. The formation rate of the fluorescent adduct was improved with an increase of pH from 7.01 to 9.50, and the highest fluorescence intensity was obtained at pH 9.50. This is coincident with the previously published interpretation that a basic medium is required to keep the thiol and amine analyte in the unprotonated form for reaction (Pastor-Navarro et al. 1998). However, the signal was dramatically reduced when the pH value increased from 10.01 to 12.02, probably due to partial hydrolysis of the *o*-phthalaldehyde. In addition, at high pH, the possibility of reaction of *S*-nitrosocaptopril with the thiolate captopril anion (pK_{SH} of 9.8) to form the S-S dimer is more likely (Sexto and Iglesias 2011).

In this study, the influences of captopril and glycine ratio on the derivatization reaction were investigated. In theory, the mole ratio of derivatization among *o*-phthalaldehyde, captopril and glycine is 1:1:1 according to the reaction mechanism, shown in Figure 1. During the 6 h reaction time, the fluorescent product was monitored at each hour interval. The results are shown in Figure 9(A,B) and indicate the derivatization did not occur when there is no captopril or glycine in the reaction mixture. The fluorescence intensity increased linearly with the increase of captopril or glycine. The ratio of captopril to the other reactants is less than or equal to 1 due to its consumption by nitrite in this study. The linear relation can be fit for the determination of nitrite using the proposed indirect method. Therefore, the ratio of 1:1:1 among *o*-phthalaldehyde, captopril and glycine was chosen for the following studies.

The formation rate and fluorescence intensity of the product depends not only on the ratio of *o*-phthalaldehyde, captopril, and glycine, but also on the presence of other components in the reaction mixture, like the buffer. Thus, we investigated the effect of the buffer concentration on the fluorescence intensity during the time course of the *o*-phthalaldehyde induced fluorescence reaction and the pH of the borate buffer was fixed at 9.50. Different concentration of borate buffers including 3, 5, 10, 20, 40, 60, and 100 mM were prepared and adjusted by NaOH solution. During the 6-h reaction time, the fluorescent products were monitored at each hour interval. The fluorescence measurements trend with buffer concentration was varied but the results indicated that

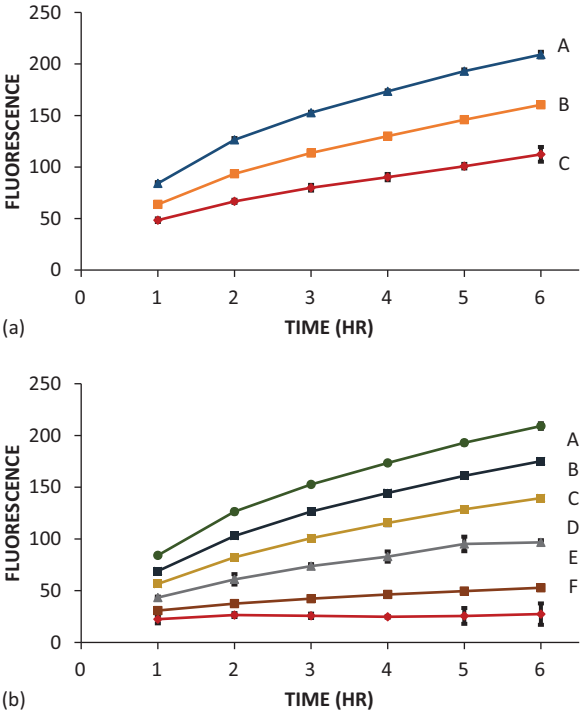

Figure 9. (A) Fluorescence as a function of time for the reaction of *o*-phthalaldehyde, captopril, and glycine. The reactant ratio is 1:1:*x* where *x* is (A) 1 (blue triangles), (B) 0.6 (orange squares), and (C) 0.3 (red circles). (B) Fluorescence as a function of time for the reaction of *o*-phthalaldehyde, glycine, and captopril. The respective reactant ratio is 1:1:*x* where *x* is (A) 1 (green circles), (B) 0.8 (blue squares), (C) 0.6 (yellow squares), (D) 0.4 (gray triangles), (E) 0.2 (brown squares), and (F) 0 (red diamonds).

the highest buffer concentration of 100 mM was best. Concentrations above this value were not tried due to solubility concerns.

Both the reaction rate and the yield of the fluorescent product depend strongly on the temperature of the reaction medium. The effect of temperature from 5 °C to 50 °C on the fluorescence intensity with concentration of sodium tetraborate fixed at 0.1 M was studied for this method. During the reaction time of 6 h, temperature was held constant. The data are shown in Figure 10. Decreased fluorescence was displayed with an increase of the reaction temperature from 15 °C to 21 °C. Interval conversion of the fluorescing derivative is the likely cause of this decreased fluorescence. The phenomenon is markedly apparent at 30 °C and the derivative almost does not fluoresce at 50 °C. In the present method, the optimum reaction temperature was chosen to be 10 °C. However, a salting out effect was observed at low temperatures below 10 °C due to marginal solubility of sodium tetraborate (Apelblat and Manzurola 2003).

In our study, we investigated the effect of the reaction time on the fluorescence intensity within a range of 60–2,400 min at 10 °C. The results are shown in Figure 11. The fluorescent intensity of the product rose rapidly with increasing reaction time from 60 to about 600 min. A slightly increase was observed when the reaction time was extended

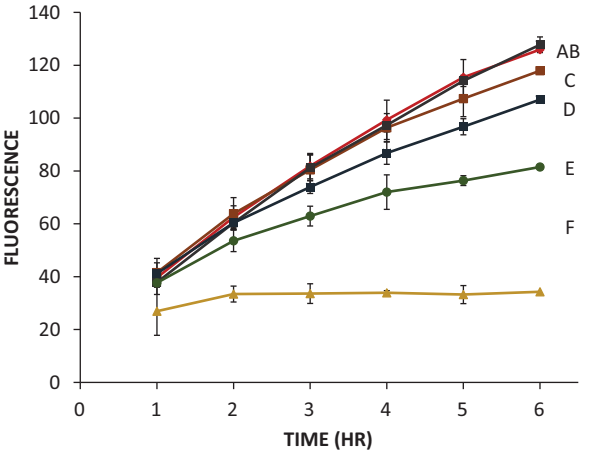

Figure 10. Fluorescence of the captopril-*o*-phthalaldehyde–glycine reaction as a function of time and temperature: (A) black squares 5 °C, (B) red diamonds 10 °C, (C) brown squares 15 °C, (D) blue squares 21 °C, (E) green triangles 30 °C, and (F) yellow triangles 50 °C.

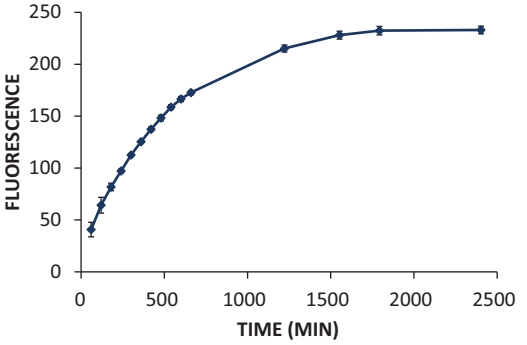

Figure 11. Fluorescence as a function of reaction time at 10 °C for the captopril-*o*-phthalaldehyde-glycine system.

from 600 to 1,222 min. Beyond this time, nearly the same fluorescent intensity was obtained. The 1:1:1 ratio of captopril, *o*-phthalaldehyde, and glycine, pH 9.5 0.1 M borate buffer, 10 °C and 24 h (or at least overnight) are the chosen fluorescence reaction conditions.

Interference studies

Interference studies were carried out to evaluate the selectivity of this indirect fluorescence detection method for nitrite. Two interference studies were performed to examine interactions between individual interferents and captopril. In the first interference study, eight common cationic interferences, including two alkali metals, three alkaline earths, and three transition metals, were reacted at both equimolar concentrations and at 10-fold excess, as compared to captopril in the absence of the metal nitrite. In

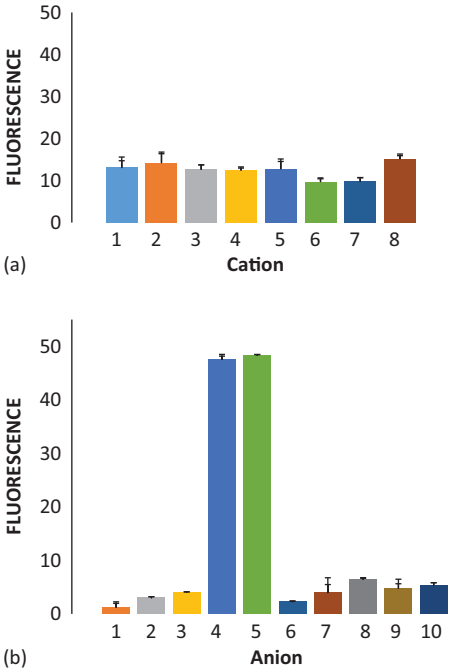

Figure 12. (A) Effect of cation interferences on the nitrite-captopril and o-phthalaladehyde-captopril-glycine reaction using 50 nM nitrite and 50 nM nitrate salts: (1) Na^{+}, (2) K^{+}, (3) Sr^{2+}, (4) Pb^{2+}, (5) Mg^{2+}, (6) Ca^{2+}, (7) Zn^{2+}, and (8) Fe^{3+}. (B) Effect of anion interferences on the nitrite-captopril and o-phthalaladehyde-captopril-glycine reaction using 50 nM nitrite and 50 nM sodium salts: (1) Cl^{-}, (2) Br^{-}, (3) I^{-}, (4) IO_3^{-}, (5) IO_4^{-}, (6) ClO_4^{-}, (7) SO_3^{2-}, (8) $S_2O_3^{2-}$, (9) SO_4^{2-}, and (10) PO_4^{3-}.

Figure 12(A), the environmentally relevant cations caused a very weak fluorescence difference, showing these cations did not interfere with the reaction between captopril and nitrite. The selectivity was higher for nitrite by a factor of 20 even when these cations were the same concentration as nitrite. Cations caused less than a 5% change in the signal. This is in contrast to spectrophotometric methods using azo dye formation, which suffer from mainly Cu(II), Co(II), and Fe(III) interferences.

In the second interference study, 10 common anionic interferences, including sodium salts of chloride, bromide, iodide, iodate, periodate, perchlorate, sulfite, sulfate, thiosulfate, and phosphate were selected and reacted at both equimolar concentrations and at 10-fold excess, as compared to captopril in the absence of sodium salt. The results displayed the same tendency between equimolar concentration and 10-fold excess of interferences. As shown in Figure 12(B), most anions except iodate and periodate also caused little interference for nitrite determination. When the concentration of nitrite and sodium iodate or sodium periodate was 50 nM and the captopril concentration was 150 nM, the fluorescent value decreased about 25% as compared to the absence of sodium iodate or sodium periodate. When the concentration of sodium iodate and sodium periodate is 500 nM and captopril and nitrite were constant at 50 nM, there was no fluorescent signal.

It has been reported that compounds containing -SH groups, like captopril, are quantitatively oxidized to sulfonic acid ($-RSO_3H$) derivatives by mild oxidants, like iodate,

with reduction of iodate to iodide (Ahmed 2013). It was different with the reaction of nitrite with captopril, which could form a pink product. The iodate and periodate ion can be easily reduced by some metal reduction regents such as Zn, Sn^{2+}. The presence of common environmentally relevant interferents at high concentration that decreased the absorbance of nitrosocaptopril was attributed to primarily ionic strength effects.

Linearity and detection limits

In order to evaluate the indirect method, linearity, detection limit, and precision studies were done. The calibration curve was generated using the nitrite-dependent fluorescence emission signal at 450 nm. Each point on the calibration curve corresponded to the mean value obtained from three independent fluorescence intensity measurements. The fluorescence intensity was found to linearly decrease with increasing nitrite concentration from 0 to 140 nM (6.4 ppb). The linear least square regression analysis equation (Figure 13(A)) corresponds to $y = -1.100(x) \pm 0.0267 + 171.3 \pm 2.57$, and the correlation coefficient (R^2) is 0.9991. Relative standard deviations of the slope and intercept were 2.4% and 1.5%, respectively.

The limit of detection and the limit of quantification were estimated in accordance with 3 times and 10 times the baseline noise level divided by the slope. The baseline noise was the average of 10 times the detector response for a blank solution. The limit of detection and the limit of quantification were 0.8 and 2.5 nM (0.037 and 0.115 ppb,

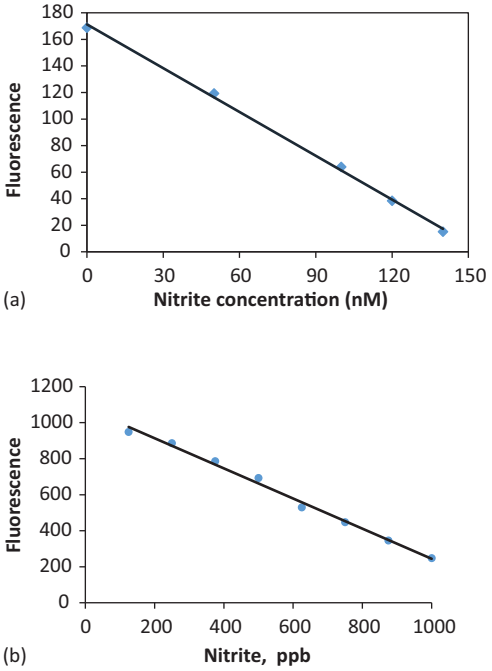

Figure 13. (A) Linearity of the nitrite-dependent fluorescence intensity using the low temperature 24-hour reaction. The calibration relationship is $y = -1.100(x) \pm 0.0267 + 171.3 \pm 2.57$, $R^2 = 0.9991$. (B) Linearity of the nitrite-dependent fluorescence intensity using the room temperature 2 h reaction (procedure 2). The calibration relationship is $y = -0.8368 \pm (x) + 1081\pm$. $R^2 = 0.9932$.

Table 1. Intraday and interday precision for the determination of nitrite using the optimum conditions described in procedure 1.

Number	Fluorescence intensity ($n = 6$)		
	First day	Second day	Third day
1	126.14	108.72	101.57
2	127.21	107.34	109.42
3	129.21	108.75	109.66
4	125.41	110.66	109.15
5	128.56	111.05	110.03
6	128.02	115.08	114.87
Intraday precision (relative standard deviation %)	1.14	2.47	3.92
Interday precision (relative standard deviation %)	7.85		

respectively). In our study, the limit of detection was similar to those reported previously in two fluorescence studies (Axelrod and Engel 1975, Wang et al. 2000) and better than most using commercially available reagents.

The precision of the method was evaluated under optimized conditions by using a standard aqueous solution containing 10 nM nitrite. For intraday precision measurements, six parallel samples were scanned and the relative standard deviation increased from 1 to 4% for days 1, 2, and 3. For inter-day precision measurements, the fluorescence values of 18 parallel samples distributed over these three days were monitored and the relative standard deviation was 7.85%. The specific data are listed in Table 1.

To evaluate the currently developed method, the recoveries of the nitrite quality control (samples spiked at different levels (10, 60, and 120 nM) in distilled deionized water were obtained. Each concentration level was repeated six times. The recoveries were 98.89% at low concentrations (relative standard deviation 1.68%), 97.27% at medium concentrations (relative standard deviation 3.41%), and 94.35% at high concentrations (relative standard deviation 6.96%), respectively. The nitrite concentrations of three different environmental water samples were found to be 4.7, 11.3, and 16.4 μM. These values are reasonable compared to a previous nitrite study of environmental water indicating about 1–20 μM levels (Wang et al. 2000, Aydin et al. 2005).

In addition, the conversion of nitrate to nitrite in blended spinach due to microbial nitrate reductase activity could be followed as a function of time. Because detection limit was not a concern, the more rapid procedure 2 was used. The fluorescence intensity was found to be a linear decrease with increasing nitrite from about 100 to 1,000 ppb (2.17–21.7 μM). The linear least square regression analysis equation (Figure 13(B)) corresponds to $y = -0.869 \pm 0.0285\ (x) + 1106 \pm 19.2$, and the correlation coefficient (R^2) is 0.9932. Relative standard deviations of the slope and intercept were 3.3% and 1.7%, respectively. The limit of detection and the limit of quantification were estimated in accordance with three times and ten times the standard deviation of the intercept divided by the slope and found to be 66.1 and 220 ppb, respectively. These values are about 200 times higher than the corresponding limit of detection and limit of quantification values determined the same way with procedure 1. Based on a literature search, the formation of nitrite in green vegetables as a function of time is not a common study.

The maximum formation of nitrite was noted at 40 h (Figure 14) which is slower than a recent previous study also done at room temperature (Watanabe and Yamasaki 2017). Possibly differences in the source of spinach samples or in the sample

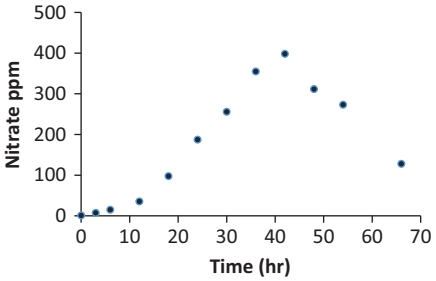

Figure 14. Formation of nitrite (mg/kg spinach) from nitrate in an aqueous spinach blend as function of time.

Table 2. Fluorometric methods for nitrite using commercially available reagents.

Reagent(s)	Reaction(s)	Detection limit (μM)	Linearity (μM)	Reference
Murexide	Nitrosation (quenching)[a]	0.01	0.1–21.7	Biswas, Chowdhury, and Ray (2004)
Rhodamine 110	Nitrosation (quenching)[a]	0.0007	0.01–0.3	Zhang et al. (2003)
Tryptophan	Nitrosation (quenching)[a]	0.022	0.22–4.3	Jie, Yang, and Meng (1993)
Indole	Nitrosation (quenching)[a]	0.054	0.22–13	Jie et al. (1999)
Acetaminophen	Nitrosation + OH^- (fluorescence)[a]	0.059	1.7–28	Helaleh and Korenaga (2000)
Aminofluorescein	Diazotization[b]	0.001	0.005–10	Axelrod and Engel (1975)
Neutral Red	Diazotization[b]	0.2	0.9–4.3	Li et al. (2003)
Folic acid	Diazotization[b]	0.018	0.05–32	Lu et al. (2015)
2,3-Diaminonaphthalene	Triazole[c]	0.02	0.02–10.0	Nussler et al. (2006)
5,6-Diamino-1,3-naphthalene disulfonic acid	Triazole[c]	0.002	0.017–2.4	Wang et al. (2000)
o-Phenylenediamine	Triazole[c]	0.3	0.9–17.4	Guo et al. (2013)
Captopril (RSH), *o*-phthalaldehyde, glycine	S-nitrosation, remaining RSH detection[d]	0.0008	0.0025–0.140	This method

[a]R–NH →RN–NO.
[b]$RNH_3^+Cl^-$ → [RN=N^+Cl^-] → RN = NOH.
[c]Aromatic diamine→ Aromatic triazole cyclization.
[d]S-nitrosation, remaining thiol detected.

preparation procedure are contributing reasons. We found the maximum value of nitrite formed was 400 mg/kg spinach which is comparable to that previously reported at 350 mg/kg (Watanabe and Yamasaki 2017). We have repeated this formation of nitrite in spinach study using the captopril-nitrite ultraviolet flow injection method recently developed by us. We found the maximum value of nitrite formed was 400 mg/kg spinach at 48 h, quite similar to our original study as shown in Figure 14.

Comparison to other fluorescence methods and potential future work

Table 2 shows a comparison of our method to other fluorescence methods for nitrite that use commercially available reagents. Our detection limit and linearity are generally better, at least comparable, to those reported previously, particularly to the

2,3-diaminonaphthalene methods which tend to dominant the literature. However, our analysis time is long in order to achieve these analytical figures of merit.

In the future, several other methods using this general approach could be developed. *o*-Phthalaldehyde could be substituted for naphthalenedialdehyde to provide a longer wavelength emission spectrum and possibly improved selectivity. Development of thiol sensing reagents is an active research area and could replace the *o*-phthaladehyde-thiol-amine as the second reaction. In particular, a coumarin derivative substituted with an unsaturated malononitrile moiety can react with a thiol, losing the quenching malononitrile group (Yin et al. 2013). A probe synthesized from ethanoylcoumarin and terephthaladehyde has been shown to be an effective fluorescent derivatizing agent for cysteine (Yue et al. 2017). Fluorescein mono- and di-aldehyde compounds have been used to react with cysteine or homocysteine to give both a color change and a fluorescence quenching response (Barve et al. 2014).

Conclusions

We offer another approach using safe, commercially available and more inexpensive reagents as compared to conventional procedures for the fluorescence determination of nitrite. The method is based on two reactions. Nitrite is first reacted with captopril to form the non-fluorescent nitroso compound. Secondly the residual captopril is then allowed to react with glycine and *o*-phthalaldehyde. Optimization included captopril as the thiol reagent, pH 1 and 40 °C for the first reaction and then the amino acid glycine, a 1:1:1 ratio of captopril, *o*-phthalaldehyde, and glycine, pH 9.5, 0.1 M borate buffer, 10 °C for the second reaction. Eight common cations and eight of ten anions were shown to have little effect on the fluorescence signal. The limits of detections and quantitation of nitrite were 0.8 and 2.5 nM, respectively, with linearity to 140 nM for procedure 1. Recoveries ranged from 94% to 99% depending on nitrite concentration with intraday and interday relative standard deviation precision of 1–4% and 7.85%, respectively. Three real water samples were also successfully analyzed for nitrite and the conversion of nitrite from nitrate in a green vegetable was easily followed. These results showed this method is flexible in application and easily adapted using procedure 2 for following nitrite formation in green vegetables such as spinach.

References

Ahmed, N. R. 2013. Indirect spectrophotometric determination of captopril in pharmaceutical tablets and spiked environmental samples. *Iraqi National Journal of Chemistry* 49:1–11.

Apelblat, A., and E. Manzurola. 2003. Solubilities and vapour pressures of saturated aqueous solutiojs of sodium tetraborate, sodium carbonate, and magnesium sulfate and freezing-temperature lowerings of sodium tetraborate and sodium carbonate. *Journal of Chemical Thermodynamics* 35 (2):221–8.

Axelrod, H. D., and N. A. Engel. 1975. Fluorometric-determination of sub-nanogram levels of nitrite using 5-aminofluorescein. *Analytical Chemistry* 47 (6):922–4.

Aydın, A., O. Ercan, and S. Taşcıoğlu. 2005. A novel method for the spectrophotometric determination of nitrite in water. *Talanta* 66 (5):1181–6.

Bartsch, H., E. Hietanen, and C. Malaveille. 1989. Carcinogenic nitrosamines: Free radical aspects of their action . *Free Radical Biology & Medicine* 7 (6):637–44.

Barve, A., M. Lowry, J. O. Escobedo, K. T. Huynh, L. Hakuna, and R. M. Strongin. 2014. Differences in heterocycle basicity distinguish homocysteine from cysteine using aldehyde-bearing fluorophores. *Chemical Communications* 50 (60):8219–22.

Biswas, S., B. Chowdhury, and B. C. Ray. 2004. A novel spectrofluorimetric method for the ultra trace analysis of nitrite and nitrate in aqueous medium and its application to air, water, soil, and forensic samples. *Talanta* 64 (2):308–12.

Brückner, H., M. Langer, M. LüPke, T. Westhauser, and H. Godel. 1995. Liquid-chromatographic determination of amino-acid enantiomers by derivatization with *o*-phthaldialdehyde and chiral thiols – applications with reference to food science. *Journal of Chromatography A* 697 (1–2):229–45.

Büldt, A., and U. Karst. 1999. Determination of nitrite in waters by microplate fluorescence spectroscopy and HPLC with fluorescence detection. *Analytical Chemistry* 71 (15):3003–7.

Cai, M., X. Chai, X. Wang, and T. Wang. 2017. An acid-inert fluorescent probe for the detection of nitrite. *Journal of Fluorescence* 27 (4):1365–71.

Concha-Herrera, V., J. R. Torres-Lapasio, and M. C. Garcia-Alvarez-Coque. 2004. Chromatographic determination of thiols after pre-column derivatization with *o*-phthaldehyde and isoleucine. *Journal of Liquid Chromatography & Related Technologies* 27 (10):1593–609.

Dashwood, R. H. 1998. Indole-3-carbinol: Anticarcinogen or tumor promoter in brassica vegetables? *Chemico-Biological Interactions* 110 (1–2):1–5.

Green, L. C., D. A. Wagner, J. Glogowski, P. L. Skipper, J. S. Wishnok, and S. R. Tannenbaum. 1982. Analysis of nitrate, nitrite, and [N-15]-labeled nitrate in biological fluids. *Analytical Biochemistry* 126 (1):131–8.

Guo, X. F., H. Wang, Y. H. Guo, Z. X. Zhang, and H. S. Zhang. 2009. Simultaneous analysis of plasma thiols by high-performance liquid chromatography with fluorescence detection using a new probe, 1,3,5,7-tetramethyl-8-phenyl-(4-iodoacetamido)difluoroboradiaza-s-indacene. *Journal of Chromatography A* 1216 (18):3874–80.

Guo, Y. X., Q. F. Zhang, X. C. Shangguang, and G. D. Zhen. 2013. Spectrofluorimetric determination of trace nitrite with *o*-phenylenediamine enhanced by hydroxypropyl-beta-cyclodextrin. *Spectrochimca Acta A* 101:107–11.

Hadjmohammadi, M. R., K. Kamel, and F. K. Nezhad. 2008. Determination of captopril in human plasma with precolumn derivatization using solid phase extraction and HPLC. *Journal of the Iranian Chemical Society* 5 (2):324–7.

Helaleh, M. I. H., and T. Korenaga. 2000. Fluorometric determination of nitrite with acetaminophen. *Microchemical Journal* 64 (3):241–6.

Higdon, J. V., B. Delage, D. E. Williams, and R. H. Dashwood. 2007. Cruciferous vegetables and human cancer risk: Epidemiologic evidence and mechanistic basis. *Pharmacological Research* 55 (3):224–36.

Jie, N. Q., J. H. Yang, and F. Q. Meng. 1993. Fluorimetric determination of nitrite. *Talanta* 40 (7):1009–11.

Jie, N. Q., D. L. Yang, Q. B. Jiang, Q. Zhang, and L. Wei. 1999. A fluorescence quenching method for the determination of nitrite with indole. *Microchemical Journal* 62 (3):371–6.

Kok, R. J., J. Visser, F. Moolenaar, D. de Zeeuw, and D. K. Meijer. 1997. Bioanalysis of captopril: Two sensitive high-performance liquid chromatographic methods with pre- or postcolumn fluorescent labeling. *Journal of Chromatography. B, Biomedical Sciences and Applications* 693 (1):181–9.

Lapat, A., L. Szekelyhidi, and I. Hornyak. 1997. Spectrofluorimetric determination of 1,3,5-trinitro-1,3,5-triazacyclohexane (hexogen, RDX) as a nitramine type explosive. *Biomedical Chromatography* 11 (2):102–4.

Li, H., C. J. Meininger, and G. Y. Wu. 2000. Rapid determination of nitrite by reversed-phase high-performance liquid chromatography with fluorescence detection. *Journal of Chromatography B* 746 (2):199–207.

Li, R., J. C. Yu, Z. Jiang, R. Zhou, and H. Liu. 2003. A solid-phase fluorescent quenching method for the determination of trace amounts of nitrite in food with neutral red. *Journal of Food and Drug Analysis* 11:251–7.

Liang, S. C., H. Wang, Z. M. Zhang, and H. S. Zhang. 2005. Determination of thiol by high-performance liquid chromatography and fluorescence detection with 5-methyl-(2-(m-iodoacetylaminophenyl)benzoxazole. *Analytical and Bioanalytical Chemistry*381 (5):1095–100.

Lu, L., C. Chen, D. Zhao, F. Yang, and X. Yang. 2015. A simple and sensitive assay for the determination of nitrite using folic acid as the fluorescent probe. *Analytical Methods* 7(4):1543–8.

Material Safety Data Sheet 2,3-Diaminonaphthalene. 2017. https://fscimage.fishersci.com/msds/76602.htm (accessed March 7, 2017).

Mukai, Y., T. Togawa, T. Suzuki, K. Ohata, and S. Tanabe. 2002. Determination of homocysteine thiolactone and homocysteine in cell cultures using high-performance liquid chromatography with fluorescence detection. *Journal of Chromatography B-Analytical Technologies in the Biomedical Life Sciences* 767 (2):263–8.

Nolin, T. D., M. E. McMenamin, and J. Himmelfarb. 2007. Simultaneous determination of total homocysteine, cysteine, cysteinylglycine, and glutathione in human plasma by high-performance liquid chromatography: Application to studies of oxidative stress. *Journal of Chromatography B-Analytical Technologies in the Biomedical Life Sciences* 852 (1–2):554–61.

Nussler, A. K., M. Glanemann, A. Schirmeier, L. Liu, and N. Nussler. 2006. Fluorometric measurement of nitrite/nitrate by 2,3-diaminonaphthalene. *Nature Protocols* 1 (5):2223–6.

Ogasawara, Y., Y. Mukai, T. Togawa, T. Suzuki, S. Tanabe, and K. Ishii. 2007. Determination of plasma thiol bound to albumin using affinity chromatography and high-performance liquid chromatography with fluorescence detection: Ratio of cysteinyl albumin as a possible biomarker of oxidative stress. *Journal of Chromatography B-Analytical Technologies in the Biomedical Life Sciences* 845(1):157–63.

Pandurangappa, M., and Y. Venkataramanappa. 2011. Quantification of nitrite/nitrate in food stuff samples using 2-aminobenzoic acid as a new amine in diazocoupling reaction. *Food Analytical Methods* 4 (1):90–9.

Pastor-Navarro, M. D., R. Porras-Serrano, R. Herraez-Hernandez, and P. Campins-Falco. 1998. Automated determination of amphetamine enantiomers using a two-dimensional column-switching chromatographic system for derivatization and separation. *The Analyst* 123 (2):319–24.

Radomski, J. L., E. Brill, W. B. Deichman, and E. M. Glass. 1971. Carcinogenicity testing of N-hydroxy and other oxidation and decomposition products of 1- and 2-naphthylamine. *Cancer Research* 31:1461–7.

Scaffidi, J. P., M. A. Porche, Z. Guo, Y. Li, A. Ali, and N. D. Danielson. 2015. Determination of nitrite using captopril by UV spectrophotometry and flow injection analysis. PittCon poster. New Orleans, LA.

Sexto, A., and E. Iglesias. 2011. S-nitrosocaptopril formation in aqueous acid and basic medium. A vasodilator and angiotensin converting enzyme inhibitor. *Organic & Biomolecular Chemistry* 9 (20):7207–16.

Shen, Y., Q. Zhang, X. Qian, and Y. Yang. 2015. Practical assay for nitrite and nitrosothiol as an alternative to the Griess assay or the 2,3-diaminonaphthalene assay. *Analytical Chemistry* 87 (2):1274–80.

Sobhanardakani, S., A. Farmany, S. Abbasi, J. Cheraghi, and R. Hushmandfar. 2013. A new catalytic-spectrophotometric method for quantification of trace amounts of nitrite in fruit juice samples. *Environmental Monitoring and Assessment* 185 (3):2595–601.

Sugimura, T. 2000. Nutrition and dietary carcinogens. *Carcinogenesis* 21 (3):387–95.

Wang, H., W. Yang, S. C. Liang, Z. M. Zhang, and H. S. Zhang. 2000. Spectrofluorimetric determination of nitrite with 5,6-diamino-1,3-naphthalene disulfonic acid. *Analytica Chimica Acta* 419 (2):169–73.

Wang, Q.-H., L.-J. Yu, Y. Liu, L. Lin, R.-G. Lu, J.-P. Zhu, L. He, and Z.-L. Lu. 2017. Methods for the detection and determination of nitrite and nitrate: A review. *Talanta* 165:709–20.

Watanabe, N. S., and H. Yamasaki. 2017. Dynamics of nitrite content in fresh spinach leaves: Evidence for nitrite formation caused by microbial nitrate reductase activity. *Journal of Nutrition and Food Science* 7:1–6.

Wiersma, J. H. 1970. 2,3-Diaminonaphthalene as a spectrophotometric and fluorometric reagent for the determination of nitrite ion. *Analytical Letters* 3 (3):123–32.

Yue, Y.,. F. Huo, P. Ning, Y. Zhang, J. Chao, X. Meng, and C. Yin. 2017. Dual-site fluorescent probe for visualizing the metabolism of cys in living cells. *Journal of the American Chemical Society* 139 (8):3181–5.

Yin, C., F. Huo, J. Zhang, R. Martinez-Manez, Y. Yang, H. Lv, and S. Li. 2013. Thiol-addition reactions and their applications in thiol recognition. *Chemical Society Reviews* 42 (14):6032–59.

Zhang, X., H. Wang, N. N. Fu, and H. S. Zhang. 2003. A fluorescence quenching method for the determination of nitrite with rhodamine 110. *Spectrochimica Acta. Part A, Molecular and Biomolecular Spectroscopy* 59 (8):1667–72.